J. Opt. A: Pure Appl. Opt. **9** (2007) 872–876 doi:10.1088/1464-4258/9/10/017

A study of the porosities of polymer nanoporous films using numerical simulations and experimental methods

Z Y Yang[1] and M Zhao[2]

[1] State Key Laboratory of Laser Technology, Huazhong University of Science and Technology, Wuhan, Hubei 430074, People's Republic of China
[2] Wuhan National Laboratory for Optoelectronics, Huazhong University of Science and Technology, Wuhan, Hubei 430074, People's Republic of China

E-mail: yppzm@yahoo.com.cn (Z Y Yang)

Received 2 July 2007, accepted for publication 17 July 2007
Published 5 September 2007
Online at stacks.iop.org/JOptA/9/872

Abstract
In this study, the finite difference time domain (FDTD) method was used to analyze light propagation in polymer nanoporous films. Compared with some theoretical models, it is found that the composite medium in series model is consistent with the results calculated by the FDTD method. In order to verify the theoretical model, we also fabricated several polymer nanoporous films, and obtained their effective indices of refraction and porosities with an ellipsometer and scanning electronic microscope (SEM), respectively. It is indicated that the composite medium in series model is also consistent with the experimental results.

Keywords: nanoporous film, nanostructured material, finite difference time domain method

1. Introduction

Nanoporous materials are of critical importance in many applications, such as catalysis [1], sensing [2], filtration and fabrication of more complex nanostructured materials [3]. In general, nanoporous films have low dielectric constants (low k) which are in demand to reduce parasitic capacitance and signal crosstalk between interconnects and improve the switching speed in ultralarge-scale integrated circuits [4]. Film porosities determine the dielectric, mechanical, thermal and chemical properties of the nanoporous films and their feasibility to be used in microelectronic technology. Increasing the porosity drives the dielectric constant down, but degrades the mechanical and chemical properties of the film. Therefore, practical methods are needed to reliably determine the porosities of nanoporous films.

Recently, advanced non-destructive methods, such as ellipsometric porosimetry (EP) [5], small-angle neutron scattering spectroscopy (SANS) combined with specular x-ray reflectivity (SXR) [6], and positron annihilation lifetime spectroscopy (PALS) [7] have been successfully applied to attain the required pore size and pore size distribution of low-k porous thin films. To our knowledge, however, few studies have been so far reported on the porosities of polymer nanoporous films.

In this work, the FDTD method was introduced to analyze the effective indices of refraction and porosities of polymer nanoporous films. We compared the FDTD calculation results with those of some theoretical methods and found that the composite medium in series model is the most consistent with the results. Furthermore, to compare with the theoretical method, polymer nanoporous films with polystyrene (PS)/poly (methyl methacrylate) (PMMA) were fabricated and analyzed with an ellipsometer and an SEM. It is indicated that the composite medium in series model is also quite consistent with the experimental results.

2. Simulations of the FDTD method

In this work, the FDTD method was used to analyze the light wave propagation in nanoporous films. Figure 1 shows part of the structure of a nanoporous film with Yee's grids [8]. In this structure, the simulated space was split into many small grids;

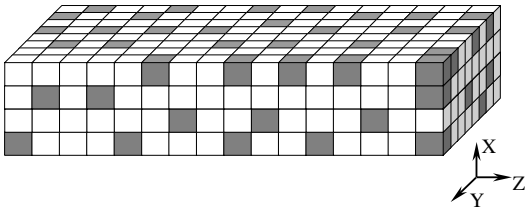

Figure 1. Structure of a nanoporous film with Yee's grids.

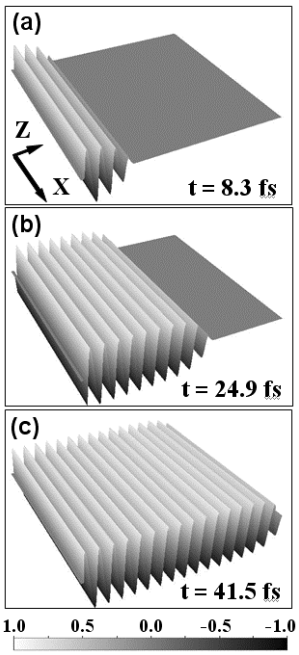

Figure 2. Electric field intensities during the propagation of light in a nanoporous film. (a) $t = 8.3$ fs, (b) $t = 24.9$ fs, (c) $t = 41.5$ fs.

each side of the grids was 25 nm. In figure 1, the white grids represent some kind of polymer with refractive index 1.46, and the black grids represent nanopores with refractive index 1. By varying the volume ratio, the porosities of the simulated nanoporous film can be changed. During the simulation, a plane wave with 750 nm wavelength was used as the light source. The direction of the light propagation was along the Z-axis and the direction of light polarization was along the Y-axis. In order to decrease the error induced by the boundary of the simulated area, a perfect matched layer (PML) was applied [9].

Figure 2 shows the distribution of the electric field intensity during the propagation of light in a nanoporous film, whose porosity is 40%. Figures 2(a), (b) and (c) show the distributions at the time $t = 8.3$, 24.9, and 41.5 fs, respectively. To calculate the effective index of refraction of the nanoporous film, the magnitude distribution of the electric field on the centerline along the Z-axis is shown in figure 3, in which ΔZ is the distance between the neighboring peaks. According to the Helmholtz equation, ΔZ must satisfy the following equations:

$$\beta \Delta Z = 2\pi, \tag{1}$$

$$\beta = n_{\text{eff}} k_0 = n_{\text{eff}}(2\pi/\lambda), \tag{2}$$

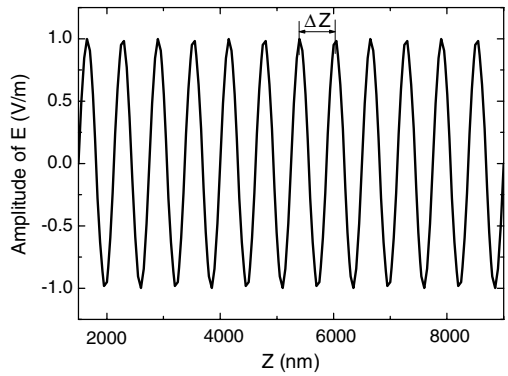

Figure 3. Magnitude distribution of the light field on the center line along the Z axis.

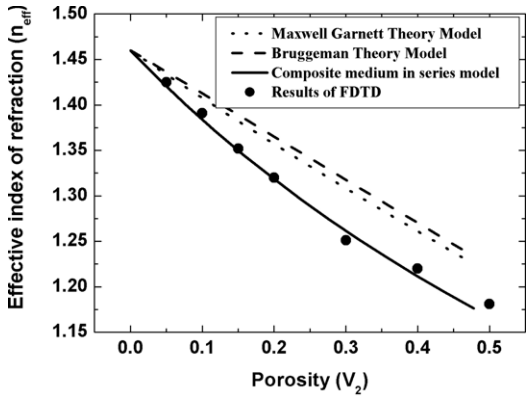

Figure 4. The comparison between the simulation results by FDTD method, the composite medium in series model, the Maxwell–Garnett theory model, and the Bruggeman theory model.

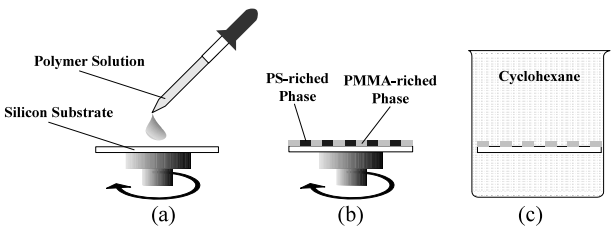

Figure 5. Procedures to fabricate nanoporous films. (a) Spin-coating, (b) nanophase separation, and (c) removal of PS.

in which β is the propagation constant; λ is the wavelength of the light source in vacuum; and n_{eff} is the effective index of refraction of the nanoporous film. Combined with equations (1) and (2), n_{eff} can be simplified as

$$n_{\text{eff}} = \lambda/\Delta Z. \tag{3}$$

In our work, we made calculations for nanoporous films with porosities of 5%, 10%, 15%, 20%, 30%, 40%, and 50%. Their effective indices of refraction are 1.425, 1.391, 1.352, 1.320, 1.251, 1.220, and 1.181, respectively. Figure 4 shows the comparison between the FDTD simulation results, the composite medium in series model (equation (4)), Maxwell–Garnett theory model (equation (5)), and Bruggeman theory

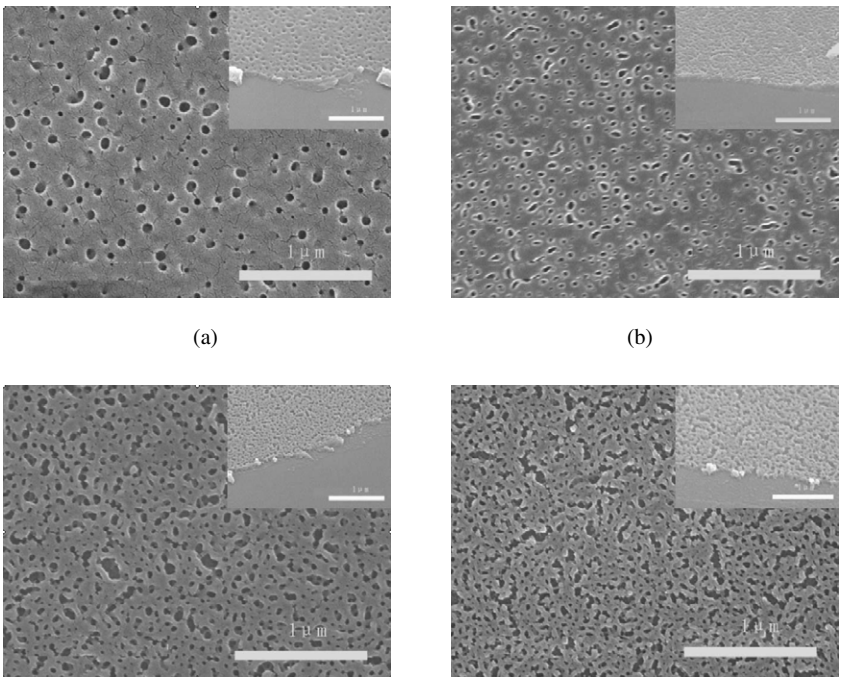

Figure 6. SEM micrographs of nanoporous polymer films with different mass ratios of PS and PMMA. PS:PMMA = (a) 50:50, (b) 55:45, (c) 60:40, and (d) 65:35.

model (equation (6)), which can be described by the following equations [10–12]:

$$n_{\text{eff}}^2 = \frac{n_1^2}{1 + (n_1^2 - 1)V_2}, \tag{4}$$

$$\frac{n_{\text{eff}}^2 - n_2^2}{n_{\text{eff}}^2 + 2n_2^2} - (1 - V_2)\frac{n_1^2 - n_2^2}{n_1^2 + 2n_2^2} = 0, \tag{5}$$

$$V_2\frac{n_1^2 + n_{\text{eff}}^2}{n_1^2 + 2n_{\text{eff}}^2} + (1 - V_2)\frac{n_2^2 - n_{\text{eff}}^2}{n_2^2 + 2n_{\text{eff}}^2} = 0, \tag{6}$$

in which n_1, n_2, V_2, and n_{eff} are the refractive index of the polymer, the refractive index of the pores (air), the porosity, and the effective index of refraction of the nanoporous film, respectively. As seen in figure 4, it is clear that the curve of the composite medium in series model is most consistent with the FDTD calculation results. Equation (4) can be deduced from the effective dielectric constant of a composite medium. The effective dielectric constant of the composite medium in series model is described by the following equations:

$$\frac{1}{\varepsilon_{\text{eff}}} = \frac{V_1}{\varepsilon_1} + \frac{V_2}{\varepsilon_2} \tag{7}$$

$$1 = V_1 + V_2, \tag{8}$$

in which ε_1 and ε_2 are the relative dielectric constant of each medium, V_1 and V_2 are the volume ratio of each medium, and ε_{eff} is the effective dielectric constant of the composite medium. It is clear that the refractive index and the dielectric constant satisfy the following equation:

$$n = \sqrt{\varepsilon}. \tag{9}$$

If n_2 is the index of pore ($n_2 \approx 1$) and V_2 is the porosity, by importing equations (8) and (9) into equation (7), equation (4) can be obtained. Since the porous size of the nanoporous film is much smaller than the wavelength of light, the film can be regarded as a structure with many units of the composite medium in series model. Therefore, the effective index of refraction of the nanoporous film can be explained by the composite medium in series model.

3. Fabrication of polymeric nanoporous films

To prove the FDTD calculation results, polymeric nanoporous films composed of PS and PMMA (Aldrich Chemical Corporation) polymers were fabricated by the nanophase separation method [13]. Both of the polymers have relatively low molecular weight, so the final pore size in the nanoporous films could be controlled to be under ~100 nm to reduce the optical scattering loss [14]. Characteristics of the polymers are listed in table 1.

The procedure of fabricating nanoporous polymer films mainly consisted of three steps: (1) spin-coating, (2) nanophase separation, and (3) PS removal in a selective solvent (shown in figure 5). An adequate amount of polymer solution was dropped onto a silicon substrate placed on a spin-coater with a rotating speed of 1000 rpm (figure 5(a)). Nanophase separation occurred due to the rotation of the spin-coater, leading to a structure composed of both PS-rich and PMMA-rich phases (figure 5(b)). The sample was then placed into cyclohexane liquid to remove the PS-rich regions (figure 5(c)). A nanoporous polymer film was finally formed. By varying the mass ratios of PS and PMMA (50:50, 55:45, 60:40, and 65:35), nanoporous films with different porosities were fabricated. Figures 6(a)–(d) show the SEM images of

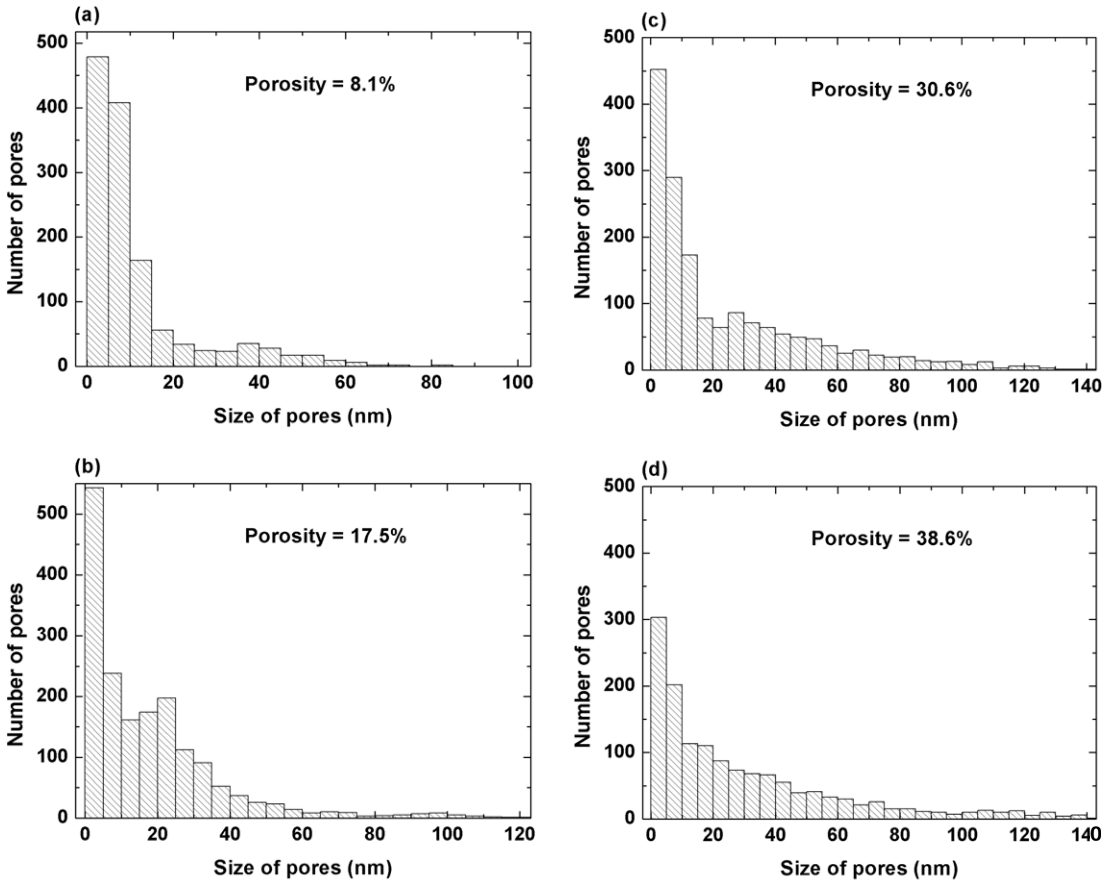

Figure 7. Porosities and size distributions of the nanoporous films. PS:PMMA = (a) 50:50, (b) 55:45, (c) 60:40, and (d) 65:35.

the nanoporous films. The inset figures are cross-sections of the SEM images. As seen from figures 6(a)–(d), it is clear that the porosities increase in sequence. Measured by an ellipsometry system (J A Woollam Co., Inc. M-2000 ellipsometer), the effective indices of refraction of the nanoporous films with PS:PMMA (50:50, 55:45, 60:40, and 65:35) at the wavelength 750 nm were 1.41, 1.32, 1.24, and 1.22, respectively. To analyze the porosities of the films, an image-processing software [15] was used to calculate the porosities from the SEM photographs. Figure 7 shows the porosities and the size distributions of the nanoporous films. Figure 8 shows the comparison between the theoretical model and the experimental results. As seen from the figure 8, it is clear that the composite medium in series model is almost consistent with the experimental results. However, there are some reasons which can explain the differences between them. First, the porosities were obtained with the SEM photographs, which can only show the patterns on the top of the films but not inside the films; second, during the fabrication of the films, some PS always remained in the nanoporous films, which can introduce some errors in the measurements of the films.

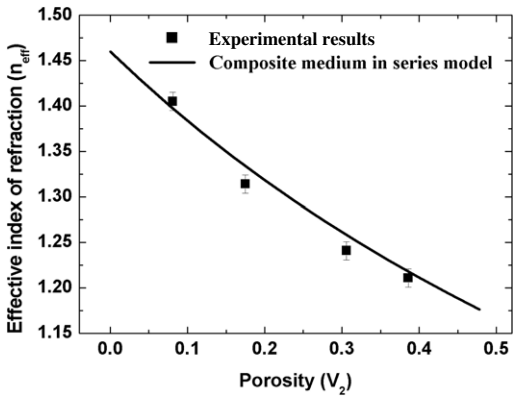

Figure 8. Comparisons between the composite medium in series model and the experimental results.

Table 1. Molecular characteristics of the polymers.

Polymer	M_w [a] (kg mol^{-1})	PD [b]
PS	10.3	1.03
PMMA	9.98	1.03

[a] Weight-averaged molecular weight.
[b] Polydispersity.

4. Conclusions

In this paper, we have introduced the FDTD method to analyze the polymer nanoporous films, and simulated the propagation of light in the films. Compared with some theoretical models, it is found that the composite medium in series model is consistent with the results calculated by the FDTD method. Furthermore, we also fabricated some polymer nanoporous

films with PS and PMMA, and obtained their effective indices of refraction and porosities with an ellipsometer and SEM, respectively. It is indicated that the composite medium in series model is also consistent with the experimental results.

Acknowledgments

The authors would like to thank Dr Y F Lu, H Wang and D Thomson for the assistance in the ellipsometry measurements, and Y X Han and Professor D R Alexander for the SEM analysis.

References

[1] Kormann H P, Schmid G, Pelzer K, Philippot K and Chaudret B 2004 Gas phase catalysis by metal nanoparticles in nanoporous alumina membranes *Z. Anorg. Allg. Chem.* **630** 1913–8

[2] Pan S L and Rothberg L J 2003 Interferometric sensing of biomolecular binding using nanoporous aluminum oxide templates *Nano Lett.* **3** 811–4

[3] Fukutani K, Tanji K, Motoi T and Den T 2004 Ultrahigh pore density nanoporous films produced by the phase separation of eutectic Al–Si for template-assisted growth of nanowire arrays *Adv. Mater.* **16** 1456–60

[4] Aoi N 1997 Novel porous films having low dielectric constants synthesized by liquid phase silylation of spin-on glass sol for intermetal dielectrics *Japan. J. Appl. Phys.* **36** 1355–9

[5] Baklanov M R, Mogilnikov K P, Polovinkin V G and Dultsev F N 2000 Determination of pore size distribution in thin films by ellipsometric porosimetry *J. Vac. Sci. Technol.* B **18** 1385–91

[6] Wu W L, Wallace W E, Lin E K, Lynn G W, Glinka C J, Ryan E T and Ho H M 2000 Properties of nanoporous silica thin films determined by high-resolution x-ray reflectivity and small-angle neutron scattering *J. Appl. Phys.* **87** 1193–200

[7] Giddley D W, Frieze W E, Dull T L, Sun J, Yee A F, Nguyen C V and Yoon D Y 2000 Determination of pore-size distribution in low-dielectric thin films *Appl. Phys. Lett.* **76** 1282–4

[8] Yee K S 1966 Numerical solution of initial boundary value problems involving Maxwell's equations in isotropic media *IEEE Trans. Antennas Propag.* **AP-14** 302–7

[9] Berenger J P 1994 A perfectly matched layer for the absorption of electromagnetic waves *J. Comput. Phys.* **114** 185–200

[10] Barrow D A, Petroff T E, Tandon R P and Sayer M 1997 Characterization of thick lead zirconate titanate films fabricated using a new sol gel based process *J. Appl. Phys.* **81** 876–81

[11] Theib W 1997 Optical properties of porous silicon *Surf. Sci. Rep.* **29** 91–192

[12] Peter K H H, Stephen T D, Friend R H and Tessler N 1999 All-polymer optoelectronic devices *Science* **285** 233–6

[13] Walheim S, Schaffer E, Mlynek J and Steiner U 1999 Nanophase-separated polymer films as high-performance antireflection coatings *Science* **283** 520–2

[14] Hattori H 2001 Anti-reflection surface with particle coating deposited by electrostatic attraction *Adv. Mater.* **13** 51–4

[15] http://rsb.info.nih.gov/ij/download.html Image J, free software for image processing